Calculation of Measurement Correlations using Point Estimate

Eduardo Caro, *Student Member, IEEE*, Juan M. Morales, *Student Member, IEEE*, Antonio J. Conejo, *Fellow, IEEE*, and Roberto Mínguez

***Abstract*—Currents, voltages and voltage-current phase angles are directly measured in substations and converted through nowadays complex measurement systems into power injection and power flow measurements. Since voltages, currents and phase angles are directly measured, they are affected by errors that are statistically independent and generally Gaussian distributed. However, power injections and flows, which are *fabricated* out of currents, voltages and phase angles, are affected by errors that are generally neither independent nor Gaussian. This paper describes a procedure to estimate the correlation matrix that identifies the dependencies among all measurements within a substation. The proposed technique that relies on Point Estimate is both accurate and computationally efficient. A realistic case study is used to compare the results obtained from the proposed technique with those obtained using a cumbersome Monte Carlo algorithm.**

***Index Terms*—Dependent measurements, Correlation coefficients, Point estimate.**

I. Introduction

A. Motivation and Aim

Currents, voltages and voltage-current phase angles are directly measured in substations. The metering systems reduce the values of currents and voltages, and then carry out the actual measurements. Meters for currents and voltages are generally independent devices affected by independent measurement errors. Moreover, these errors are generally Gaussian distributed.

Once measurements for voltages, currents and phase angles are available, the measurement system combines them mathematically to *fabricate* power injection and power flow measurements. Due to the calculations involved, the errors affecting these fabricated power measurements are generally neither independent nor Gaussian.

However, measurement processing assumes in general that all measurements are independent and Gaussian. This is the case of most state estimation algorithms that routinely consider all measurements (raw or fabricated) statistically independent and Gaussian distributed.

We provide in this paper a procedure to estimate the correlation matrix of all measurements pertaining to a substation. We show that dependencies among measurements are very significant, and that these dependencies vary very significantly with the operating conditions of the substation.

Measurement correlation matrices are important to process properly the information provided by the set of measurements available in a substation. Particularly, these matrices are important to achieve an accurate estimation of the state of the system based on the available measurement set.

The technique used to estimate the correlation matrix relies of a well-known statistical procedure known as point estimate, which provide adequate accuracy for moderate computational effort [14]–[25]. A specialized yet cumbersome Monte Carlo algorithm [26] is also provided in this paper, which is mostly used to appraise the accuracy of the point-estimate algorithm.

B. Literature Review

The technical literature is rich in references concerning substation measurements [1]–[4] and its applications, e.g., state estimation, [5]–[13]. All of these references assume that measurements are independent and Gaussian. To the best of our knowledge, no references questioning these assumptions have been found.

C. Contributions

Within the context above, the contributions of this paper are threefold:

1) To provide an efficient yet accurate technique (based on point estimate) to estimate the correlation matrix of the set of measurements within a substation.
2) To validate this point-estimate technique through a Monte Carlo algorithm.
3) To emphasize the importance of taking into account the correlation matrix to process the set of measurements of a substation, particularly for state estimation studies.

D. Paper Organization

The rest of this paper is organized as follows. Section II provides a general overview of the measuring system in a substation. In Section III a point-estimate method is developed for estimating the covariance (or variance-covariance) matrix. Section IV analyzes the characteristics of the measurement correlation matrix. Section V develops a Monte Carlo method to estimate the correlation matrix. Section VI provides and analyzes results from an illustrative case study. Finally, Section VII provides some relevant conclusions.

E. Caro, J. M. Morales, A. J. Conejo, and R. Mínguez are partly supported by Junta de Comunidades de Castilla – La Mancha through project PCI-08-0102 and by the Ministry of Education and Science of Spain through CICYT Project DPI2006-08001.

E. Caro, J. M. Morales, and A. J. Conejo are with Univ. Castilla-La Mancha, Ciudad Real, Spain (e-mails: Eduardo.Caro@uclm.es, Juan-Miguel.Morales@uclm.es, Antonio.Conejo@uclm.es).

R. Mínguez is with Univ. Cantabria, Cantabria, Spain (e-mail: R, Roberto.Minguez@unican.es)

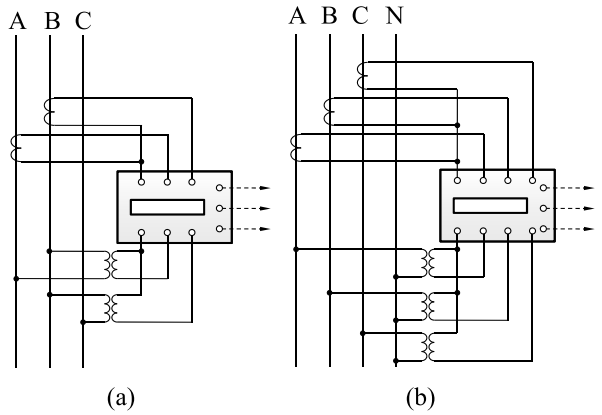

Fig. 1. Measurement connection configurations: (a) two-phase and (b) three-phase connections.

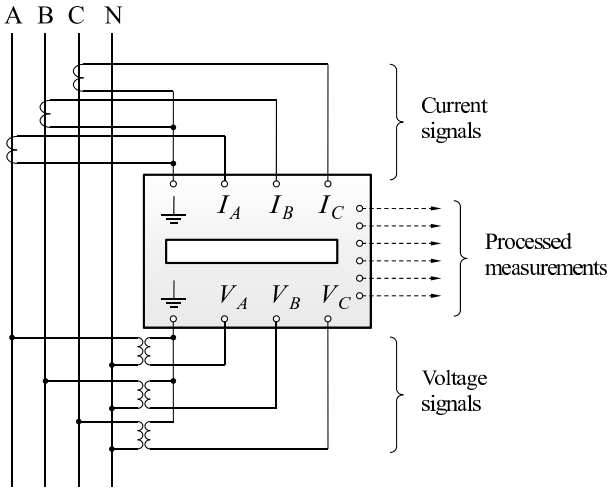

Fig. 2. Voltage signals, current signals and processed measurements.

II. Measurement Dependency

Each substation of a power system is equipped with electronic devices called Remote Terminal Units (RTUs). These units collect and process various types of measurements from the measurement system, in order to compute the values of active/reactive power flows and active/reactive power injections.

Traditionally, all these measurements are considered (i) statistically independent and (ii) Gaussian distributed. In order to check these assumptions, the measurement topology and the processing of the measured data should be studied.

A. Measurement Configuration

In this section, the measurement configuration of a substation is examined. Each measurement group is composed of a set of current and voltage transformers. These electric devices provide the current and voltage analog signals to be digitalized and processed by an electronic multifunction meter. Then, by means of a set of software routines, the multifunction meter computes the digital output data (processed measurements), using the analog input data ("raw measurements").

There are two usual configurations for the measurement group connection: the two-phase (see Fig. 1.a) and the three-phase (see Fig. 1.b) connections. In this paper, the three-phase connection is studied because it is the most common configuration in practice. However, the proposed methodology can be straightforwardly extended to the two-phase connection.

In Fig. 2, the considered measurement group configuration is depicted. Note that throughout this study the input signal errors are considered statistically independent and Gaussian-distributed. Note also that input measurements not only provide the voltage magnitude and current magnitude for each phase, but also the phase angle.

B. Multifunction Meter Equations

In this section, the internal software routines of the multifunction meter, which compute the processed measurement values, are described and studied. These computational routines are implemented in such a way that the possible presence of harmonics, imbalances or asymmetries in the network state are considered, [1]–[2]. For the sake of clarity, a sinusoidal system state is considered throughout this study, i.e., no other harmonics except the fundamental harmonic are taken into account.

Processed measurements are usually: voltage at bus i, V_i; current through line ij, I_{ij}; and active and reactive power flows for line ij, P_{ij} and Q_{ij}, respectively. The internal software routines for computing this set of processed measurements are based on the following equations:

$$V_i = \frac{V_i^A + V_i^B + V_i^C}{3} \quad (1)$$

$$I_{ij} = \frac{I_{ij}^A + I_{ij}^B + I_{ij}^C}{3} \quad (2)$$

$$P_{ij} = \sum_{f\in\{A,B,C\}} V_i^f I_{ij}^f \cos(\psi_{ij}^f) \quad (3)$$

$$Q_{ij} = \sum_{f\in\{A,B,C\}} V_i^f I_{ij}^f \sin(\psi_{ij}^f)\ , \quad (4)$$

where V_i^f is the voltage magnitude signal for phase f and bus i, I_{ij}^f, and ψ_{ij}^f are the current magnitude and voltage-current phase angle signals for phase f and line ij.

Note that equations (1)–(4) include the case of an imbalanced and/or asymmetric network state. However, for the sake of clarity, hereafter symmetric balanced working conditions are considered.

Fig. 2 and equations (1)–(4) describe the case in which the measuring group is connected to just one line. However, a substation includes generally more than one power line and, therefore, either a more complex multifunction meter should be connected, or a set of basic ones. In these cases, two new processed measurements should be defined: the active and reactive power injection of bus i, P_i and Q_i, which are computed using the following expressions:

$$P_i = \sum_{f=\{A,B,C\}} V_i^f I_i^f \cos(\psi_i^f) \quad (5)$$

$$Q_i = \sum_{f=\{A,B,C\}} V_i^f I_i^f \sin(\psi_i^f)\ , \quad (6)$$

where I_i^f and ψ_i^f are the current magnitude and voltage-current phase angle signals for phase f pertaining to the generator/load of the considered bus i, respectively.

C. Definitions

For the sake of clarity, measurements are organized into vectors, yielding the input signal vector $\boldsymbol{p}$ and processed measurement vector $\boldsymbol{z}$:

$$\begin{aligned}\boldsymbol{p} &= [p_1, \ldots, p_l, \ldots, p_\eta]^T \\ &= [V_i^f, I_i^f, \psi_i^f\, I_{ij}^f, \ldots, I_{ik}^f, \psi_{ij}^f, \ldots, \psi_{ik}^f]^T \ , \\ \boldsymbol{z} &= [z_1, \ldots, z_q, \ldots, z_\nu]^T \\ &= [V_i, I_i, I_{ij}, \ldots, I_{ik}, P_i, Q_i, P_{ij}, \ldots, P_{ik}, Q_{ij}, \ldots, Q_{ik}]^T \ .\end{aligned}$$

From (1)–(4), the transformation functional vector $\boldsymbol{F}(\cdot)$ which relates $\boldsymbol{p}$ and $\boldsymbol{z}$ is defined, satisfying is $z_q = F_q(\boldsymbol{p})$, for $q = 1, \ldots, \nu$.

D. Structure of the Correlation Matrix

The mathematical software routines (1)–(6), implemented in the multifunction meter, produce a statistical dependency structure between the processed measurements $\boldsymbol{z}$, where $\boldsymbol{z}$ which can be studied by means of the correlation matrix $\boldsymbol{\Phi}_z$.

Matrix $\boldsymbol{\Phi}_z$ is always symmetric, with diagonal elements $[\boldsymbol{\Phi}_z]_{ii}$ equal to 1, and non-diagonal elements $\{[\boldsymbol{\Phi}_z]_{ij}\,|i \neq j\}$ ranging from -1 to +1. Note that each non-diagonal element (i, j) corresponds to the statistical correlation between measurements z_i and z_j, denoted as $\rho_{z_i z_j}$. This matrix can be easily computed from the covariance matrix of the processed measurements $\boldsymbol{z}$, $\boldsymbol{C}_z$, using the following expression:

$$\rho_{z_i z_j} = \frac{c_{z_i z_j}}{\sqrt{\sigma_{z_i}^2 \sigma_{z_j}^2}} \ , \tag{7}$$

where $\sigma_{z_i}^2$ is the variance of measurement z_i (i-th diagonal element of $\boldsymbol{C}_z$), and c_{z_i, z_j} is the covariance between measurements z_i and z_j. The algorithm to estimate the measurement covariance matrix $\boldsymbol{C}_z$ is detailed in Section III below.

III. Point Estimate

A. Overview

Point estimate constitutes a methodology to obtain an approximate description of the statistical properties of the output random variables of a problem. For this, just commonly available information on the random behavior of input variables is required, specifically, their first statistical moments (e.g., mean, variance and skewness).

In particular, the aim of any point-estimate method is to compute the moments of a random variable z_q that is function F_q of η input random variables p_l, i.e.,

$$z_q = F_q(p_1, p_2, \ldots, p_l, \ldots, p_\eta). \tag{8}$$

This task is accomplished by concentrating the statistical information provided by the first few central moments of an input random variable on K points for each variable, named *concentrations*. The *k*-th concentration $(p_{l,k}, w_{l,k})$ of a random variable p_l can be defined as a pair consisting of a location $p_{l,k}$ and a weight $w_{l,k}$. The location $p_{l,k}$ corresponds to the k-th value at which function $F_q(\cdot)$ is evaluated. The weight $w_{l,k}$ is a weighting factor that quantifies the influence of this evaluation on the random behavior of the corresponding output random variable z_q.

Several point-estimate methods have been proposed in the technical literature [14]–[21]. They mainly differ on the type of variables that they can deal with (skewed or symmetric, correlated or not) and on the number of evaluations needed. From among all of them, Hong's two-point estimate method [21] has been deemed to be the most appropriate for the purpose of this paper for three reasons:

1) This method is easily implementable as analytical expressions for the determination of locations and weights are available.
2) Hong's two-point estimate method has been reported to perform satisfactorily in other electrical engineering applications, [22]–[25], especially if the number of input variables involved is relatively low and these variables can be assumed to be normally distributed [24]. Note that these two conditions are satisfied in the present study.
3) The number of simulations needed by the two-point estimate method grows linearly with the number η of input random variables. Specifically, function $F_q(\cdot)$ is to be evaluated only twice for each input variable p_l, which turns the two-point estimate method into an efficient alternative to other computationally much more costly approaches, e.g., a Monte Carlo simulation.

Next, the analytical expressions to determine the locations and weights used by the two-point estimate method are introduced.

B. Locations and Weights

Each input variable p_l is evaluated at two locations $p_{l,k}$ given by:

$$p_{l,k} = \mu_{p_l} + \xi_{l,k}\sigma_{p_l} \quad , \quad k = 1, 2 \ , \tag{9}$$

where $\xi_{l,k}$ is the standard location, and μ_{p_l} and σ_{p_l} (input data) are the mean and standard deviation of p_l.

The standard location $\xi_{l,k}$ and the weight $w_{l,k}$ are obtained by solving the non-linear system of equations [21]:

$$\left.\begin{array}{c} \sum\limits_{k=1}^{2} w_{l,k} = \frac{1}{m} \\ \sum\limits_{k=1}^{2} w_{l,k}\,(\xi_{l,k})^j = \lambda_{l,j} \quad j = 1, 2, 3 \end{array}\right\} \tag{10}$$

where $\lambda_{l,j}$ denote the j-th standard central moment of the random variable p_l with probability density function g_{p_l}, that is:

$$\lambda_{l,j} = \frac{M_j\,(p_l)}{(\sigma_{p_l})^j} \tag{11}$$

$$M_j\,(p_l) = \int_{-\infty}^{\infty} (p_l - \mu_{p_l})^j\, g_{p_l} dp_l \ . \tag{12}$$

Note that $\lambda_{l,1}$ equals zero, $\lambda_{l,2}$ equals one, and $\lambda_{l,3}$ is the skewness coefficient of p_l.

The non-linear system of equations (10) can be solved analytically and, as a result, standard locations and weights can be directly obtained from the following expressions:

$$\xi_{l,1} = \frac{\lambda_{l,3}}{2} + \sqrt{\eta + \left(\frac{\lambda_{l,3}}{2}\right)^2} \quad \xi_{l,2} = \frac{\lambda_{l,3}}{2} - \sqrt{\eta + \left(\frac{\lambda_{l,3}}{2}\right)^2} \tag{13}$$

and

$$w_{l,1} = -\frac{1}{\eta}\ \frac{\xi_{l,2}}{\xi_{l,1} - \xi_{l,2}} \qquad w_{l,2} = \frac{1}{\eta}\ \frac{\xi_{l,1}}{\xi_{l,1} - \xi_{l,2}}. \tag{14}$$

Then, taking into account the mean and standard deviation of p_l, the locations $p_{l,1}$ and $p_{l,2}$ can be computed from (9).

In the following subsection, the two-point estimate method is particularized for its application to the calculation of the measurement covariance matrix.

C. Estimation of the Measurement Covariance Matrix

The covariance matrix $\boldsymbol{C}_z$ associated to the processed measurements can be computed by using the two-point estimate method described above, where the input random variable vector $\boldsymbol{p}$, the output random variable vector $\boldsymbol{z}$ and the functional vector $\boldsymbol{F}(\cdot)$ are defined in Section II-C.

As stated in Section II-A, input random measurements are considered Gaussian-distributed, i.e. their skewness coefficient is zero. Thus, expressions (13) and (14) determining locations and weights of the two-point estimate method boil down to:

$$\xi_{l,1} = \sqrt{\eta}\ , \quad \xi_{l,2} = -\sqrt{\eta}\ , \tag{15}$$

$$w_{l,1} = \frac{1}{2\eta}\ , \quad w_{l,2} = \frac{1}{2\eta}\ . \tag{16}$$

Using (9) and (15)–(16), all concentrations $(p_{l,k}, w_{l,k})$ are obtained. Subsequently, function $\boldsymbol{F}(\cdot)$ is evaluated 2η times ($l = 1, \ldots, \eta; k = 1, 2$), yielding vector $\boldsymbol{Z}(l,k)$, whose components $Z_q(l,k)$ are computed as:

$$\begin{aligned} Z_q(l,k) &= F_q(\mu_{p_1}, \ldots, \mu_{p_{l-1}}, p_{l,k}, \mu_{p_{l+1}}, \ldots, \mu_{p_\eta}) \\ &= F_q(\mu_{p_1}, \ldots, \mu_{p_{l-1}}, \mu_{p_l} + \xi_{l,k}\sigma_{p_l}, \mu_{p_{l+1}}, \ldots, \mu_{p_\eta})\ . \end{aligned}$$

1) Calculation of diagonal terms of $\boldsymbol{C}_z$: Using weighting factors $w_{l,k}$ and $Z_q(l,k)$ values, the j-th non-cross moment of the output random variable z_q can be estimated as follows (see [24]):

$$E[z_q^j] \approx \sum_{l=1}^{\eta} \sum_{k=1}^{2} w_{l,k} (Z_q(l,k))^j\ , \tag{17}$$

where $E[\cdot]$ denotes the expectation operator.

Note that variances of the processed measurements $\sigma_{z_q}^2$, which constitute the diagonal terms of $\boldsymbol{C}_z$, can be easily computed from (17) as:

$$\sigma_{z_q}^2 = E[z_q^2] - (E[z_q])^2 = E[z_q^2] - \mu_{z_q}^2\ . \tag{18}$$

2) Calculation of non-diagonal terms of $\boldsymbol{C}_z$: Point-estimate methods were developed to compute approximately the statistical moments of the marginal distributions (non-crossed moments) pertaining to the output random variables of a system under uncertainty [14]. Nevertheless, in this paper, it is experimentally and theoretically shown (see Section VI and the Appendix, respectively) that these methods can be revised easily to estimate the covariance (second order crossed moment), $c_{z_q z_{q'}}$, between two output measurements z_q and $z_{q'}$ through the following expressions:

$$E[z_q z_{q'}] \approx \sum_{l=1}^{\eta} \sum_{k=1}^{2} w_{l,k} (Z_q(l,k) Z_{q'}(l,k))\ , \tag{19}$$

$$c_{z_q z_{q'}} = E[z_q z_{q'}] - E[z_q] E[z_{q'}]\ . \tag{20}$$

Note the analogy existing between equations (17)–(18) and (19)–(20). In the Appendix, it is shown that expressions (19)–(20) constitute a first-order approximation of the covariance $c_{z_q z_{q'}}$. Likewise, in the case study discussed in Section VI, this approximation is shown to be highly accurate for the problem tackled in this paper.

IV. Characterization of Measurement Correlations

In the previous section, a point-estimate technique is developed for estimating the measurement covariance matrix $\boldsymbol{C}_z$. On the other hand, as stated in Section II, the correlation matrix $\boldsymbol{\Phi}_z$ can be computed using $\boldsymbol{C}_z$ and equation (7). In this section, the numerical structure of this matrix is numerically explored.

Pursuing clarity and simplicity, a simple measurement system is studied: a multifunction meter connected in the three-phase configuration (as depicted in Fig. 2). It provides the following output measurements: voltage V and active/reactive power flows, P and Q, respectively.

The internal software routines of the multifunction meter have nine independent input variables, $\{V^f, I^f, \psi^f\}$ for each phase f, and three output variables, $\{V, P, Q\}$. The correlation coefficients are $\{\rho_{VP}, \rho_{VQ}, \rho_{PQ}\}$. Considering balanced symmetric working conditions, input variables are equal for each phase.

Input variables are characterized by their means and standard deviations, as a result of being considered normally distributed. Therefore, the value of each correlation coefficient is determined as a function of input parameters $\{\mu_V, \mu_I, \mu_\psi, \sigma_V, \sigma_I, \sigma_\psi\}$. Due to standard deviations are determined by measurement device accuracies, they are considered known parameters. Therefore, $\{\rho_{VP}, \rho_{VQ}, \rho_{PQ}\}$ values are studied as a function of $\{\mu_V, \mu_I, \mu_\psi\}$.

A. Analysis of the Absolute Values of the Correlations

Some general characteristics regarding how correlation absolute values evolve as input variable average values vary within typical ranges are highlighted below.

The considered variation ranges of parameters μ_V, μ_I, and μ_ψ are $[0.9, 1.1]$ (p.u.), $[0, 1.5]$ (p.u.), and $[0, 1.5]$ (rad), respectively. Observe that $1.5 \approx \pi/2$.

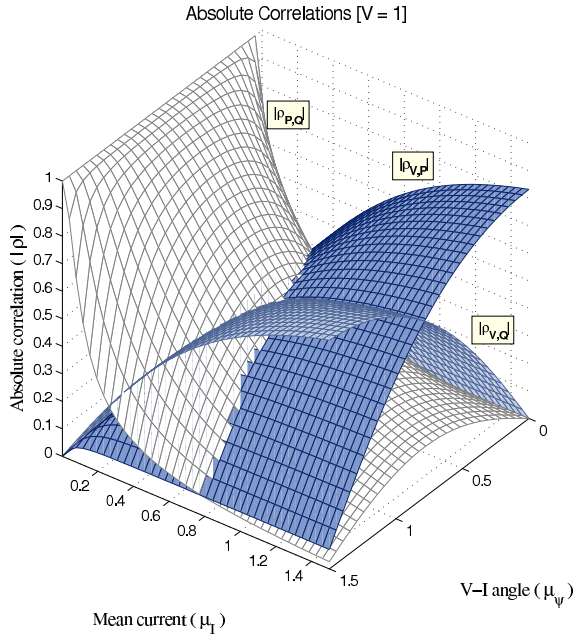

Fig. 3. Absolute correlation values $|\rho|$, for several μ_I and μ_ψ [$\mu_V = 1.0$].

For each value of $\{\mu_V, \mu_I, \mu_\psi\}$, coefficients $\{|\rho_{VP}|, |\rho_{VQ}|, |\rho_{PQ}|\}$ are computed using the proposed point-estimate technique. Considering a large number of evaluations, it has been observed that (i) mean voltage magnitude variation does not cause substantial changes in the correlation coefficients, and that (ii) the numerical relationships between $\{|\rho_{VP}|, |\rho_{VQ}|, |\rho_{PQ}|\}$ and $\{\mu_V, \mu_I, \mu_\psi\}$ can be depicted in a three-dimensional plot.

The correlation absolute values are plotted in Fig. 3 as a function of the mean current magnitude, μ_I, and mean phase angle, μ_ψ.

From Fig. 3 some trends of these coefficients can be inferred:

1) If the mean current value μ_I is low, the coefficient $|\rho_{PQ}|$ has generally a large absolute value, whereas $|\rho_{VP}|$ and $|\rho_{VQ}|$ values are close to zero.
2) If the mean current value is high, $|\rho_{VP}|$ and $|\rho_{VQ}|$ values are generally higher than the value of $|\rho_{PQ}|$.
3) Within ranges where the value of μ_I is high, $|\rho_{VP}|$ and $|\rho_{VQ}|$ values depend on μ_ψ, and the following relationships can be inferred:

$$\begin{cases} 0 = \psi & \longrightarrow & |\rho_{VP}| > |\rho_{VQ}| & = 0 \\ 0 < \psi < \frac{\pi}{4} & \longrightarrow & |\rho_{VP}| > |\rho_{VQ}| & \\ \psi = \frac{\pi}{4} & \longrightarrow & |\rho_{VP}| = |\rho_{VQ}| & \\ \frac{\pi}{4} < \psi < \frac{\pi}{2} & \longrightarrow & |\rho_{VP}| < |\rho_{VQ}| & \\ \psi = \frac{\pi}{2} & \longrightarrow & 0 = |\rho_{VP}| < |\rho_{VQ}| & \end{cases}$$

Note that Fig. 3 can be used to estimate approximately the correlation values for any bus i, once measurements $\{I_{ij}^f, \psi_{ij}^f\}$ for line ij are known.

For the sake of conciseness, note that (i) the correlation coefficient sign is not considered in this study, and (ii) the variation range for μ_ψ is rather small.

V. Monte Carlo Method

The Monte Carlo method [26] is generally applied if it is infeasible to use analytical expressions. In our case, there is no procedure to obtain the measurement correlation matrix in an exact manner. Therefore, a Monte Carlo method is used to determine approximately this matrix. Due to the fact that the Monte Carlo method is a computational algorithm which is based on repeated random sampling, its computational efficiency is particularly low. In our study, this method is used as a benchmark, to test point-estimate results.

If the correlation matrix $\mathbf{\Phi}_z$ is numerically estimated by a Monte Carlo method, its coefficients are subject to error. This error depends on the considered sample size n. In order to check point-estimate results, the confidence intervals of Monte Carlo results should be computed. Parameters r_{lo} and r_{up} define this range, satisfying:

$$\mathrm{P}[r_{lo} \leq \rho^{\mathrm{POP}} \leq r_{up}] = 1 - \alpha \ , \tag{21}$$

where ρ^{POP} is the population correlation coefficient, $1-\alpha$ is the confidence level (usually $\alpha = 0.05$), and $P[x_{lo} \leq x \leq x_{up}]$ is the probability of x being in the range of $[x_{lo}, x_{up}]$.

Hypotheses about the population correlation value ρ^{POP} can be tested using the Fisher transformation [27] applied to the sample correlation ρ. Applying this transformation, the confidence interval of ρ^{POP} are defined by $r_{lo}(n,\rho)$ and $r_{up}(n,\rho)$, through the following expressions:

$$r_{lo}(n,\rho) = \tanh\left[\frac{1}{2}\log\left(\frac{1+\rho}{1-\rho}\right) + \frac{\mathrm{erfinv}\,(\alpha-1)\sqrt{2}}{\sqrt{n-3}}\right] \tag{22}$$

$$r_{up}(n,\rho) = \tanh\left[\frac{1}{2}\log\left(\frac{1+\rho}{1-\rho}\right) - \frac{\mathrm{erfinv}\,(\alpha-1)\sqrt{2}}{\sqrt{n-3}}\right] \tag{23}$$

where $\mathrm{erfinv}(\cdot)$ is the value of the inverse error function, and ρ is the sample correlation coefficient (provided by Monte Carlo simulation). Note that these limits depend on the number of samples n and the value of the sample correlation coefficient ρ.

The Confidence Interval Width (hereafter called CIW), at a confidence level $1-\alpha$, can be computed as the difference between $r_{up}(n,\rho)$ and $r_{lo}(n,\rho)$:

$$\mathrm{CIW}(n,\rho) = r_{up}(n,\rho) - r_{lo}(n,\rho) \ . \tag{24}$$

Fig. 4 depicts the CIW values as a function of n and ρ. Note that sample size axis is logarithmical.

In order to ensure a desired tolerance in the Monte Carlo results, a minimum sample size n should be considered. Fig. 5 depicts the required sample size for several confidence interval widths and absolute correlation coefficients $|\rho|$, for a confidence level of 95% ($\alpha = 0.05$). Note, from Fig. 4–5, that the CIW is larger if $|\rho|$ is closer to zero.

VI. Case Study

In this section, the IEEE 30-bus system [28] is considered in order to (i) check the traditional assumption about Gaussian errors in processed measurements, (ii) to compute the correlation matrix using the Monte Carlo method, (iii) to compute this

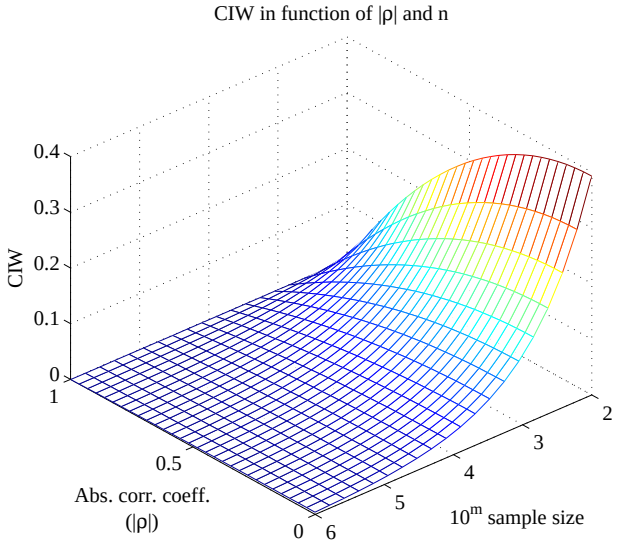

Fig. 4. Confidence interval width versus n and ρ ($\alpha = 0.05$).

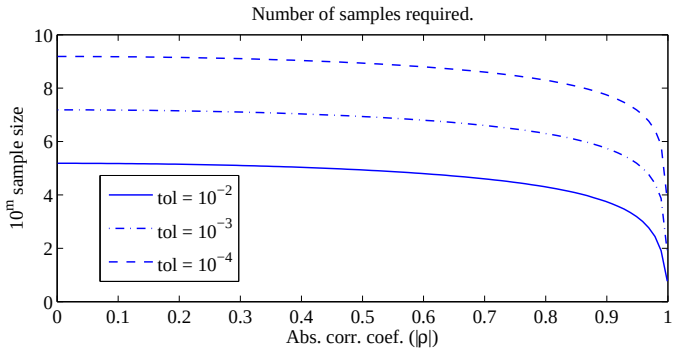

Fig. 5. Required sample size versus correlation, for several tolerances.

matrix using a point-estimate technique, (iv) to compare both methods in terms of accuracy and computational efficiency, and (v) to study the correlation coefficient values for some illustrative buses.

In this case study three realistic assumptions are considered: (i) the power system working conditions are symmetric and balanced; (ii) the measurement configuration for each multifunction meter is the three-phase connection; and (iii) the multifunction meter output data are assumed to include voltage, active/reactive power flows and active/reactive power injections.

A. Gaussian Assumption

In this subsection the traditional assumption about Gaussian-distributed measurements is examined. A converged power flow solution is considered in order to obtain the true value of each measurement. Afterwards, a random zero-mean Gaussian error (which a standard deviation characterized by the measurement device accuracy) is added to these measurements, in order to obtain realistic measurements (input data). Subsequently, processed measurements (output data) are computed using (1)–(4).

The statistical distribution of each processed measurement can be characterized by generating a large sample of measurement scenarios. This characterization can be numerical (e.g., computing its skewness and kurtosis) or graphical (e.g., plotting its probability density function, or its cumulative density function).

Considering one million of measurement scenarios, the skewness and kurtosis for the statistical distribution of each processed measurement are computed. Table I provides the statistical characterization (mean and standard deviation) for the skewness and kurtosis of each type of the processed measurement. Note that the skewness and kurtosis of a perfect Gaussian distribution are zero and three, respectively.

TABLE I
NUMERICAL CHARACTERIZATION OF THE PROCESSED MEASUREMENTS STATISTICAL DISTRIBUTIONS.

Type of measurement	Skewness		Kurtosis	
	Average	Std. Dev.	Average	Std. Dev.
V_i	-0.0003	0.0022	3.0011	0.0049
P_i	0.0001	0.0047	3.0669	0.3605
Q_i	-0.0057	0.0252	3.0697	0.3638
P_{ij}	0.0001	0.0064	3.0008	0.0046
Q_{ij}	-0.0004	0.0592	3.0604	0.3097

From Table I it can be concluded that the distribution of the processed measurements can be considered Gaussian: the average skewness is approximately zero, and the average kurtosis is slightly above three. This numerical validation as well as others graphical characterizations have been considered for all processed measurements in the 30-bus system, as well as in other realistic systems, and the obtained results are similar. Therefore, it can be concluded that the traditional assumption about Gaussian errors is realistic.

B. Monte Carlo Results

In this subsection, the Monte Carlo method is used to compute the correlation matrix $\mathbf{\Phi}_z$, used below as a benchmark for comparison purposes. For the sake of conciseness, only correlations between voltage and active power flow/injections are displayed.

As stated in Section V, the Monte Carlo method provides an accuracy level dependent on the sample size n. Considering ten million of measurement scenarios ($n = 10^7$), the CIW is approximately 10^{-3} for a confidence level of 95% (see Fig. 5).

Using the Monte Carlo (MC) method to compute $\mathbf{\Phi}_z^{\mathrm{MC}}$ at bus 1, a bus connected to buses 2 and 3 through lines 1–2 and 1–3, respectively, obtaining the following matrix:

$$\mathbf{\Phi}_z^{\mathrm{MC}} = \begin{array}{c} \\ V \\ P \\ P_{1,2} \\ P_{1,3} \end{array} \begin{array}{c} \begin{array}{cccc} V & P & P_{1,2} & P_{1,3} \end{array} \\ \begin{pmatrix} 1.0000 & 0.6126 & 0.4590 & 0.2523 \\ 0.6126 & 1.0000 & 0.2816 & 0.1544 \\ 0.4590 & 0.2816 & 1.0000 & 0.1159 \\ 0.2523 & 0.1544 & 0.1159 & 1.0000 \end{pmatrix} \end{array}$$

Using (22)–(23), lower (and upper) bounds for each correlation coefficient are estimated for a 95% confidence level, resulting the following values of $\underline{\mathbf{\Phi}_z^{\mathrm{MC}}}$ ($\overline{\mathbf{\Phi}_z^{\mathrm{MC}}}$):

$$\begin{array}{cccc} V & P & P_{1,2} & P_{1,3} \end{array} \\ \begin{pmatrix} 1.0000(1.0000) & 0.6122(0.6130) & 0.4586(0.4595) & 0.2517(0.2529) \\ 0.6122(0.6130) & 1.0000(1.0000) & 0.2810(0.2822) & 0.1538(0.1550) \\ 0.4586(0.4595) & 0.2810(0.2822) & 1.0000(1.0000) & 0.1152(0.1165) \\ 0.2517(0.2529) & 0.1538(0.1550) & 0.1152(0.1165) & 1.0000(1.0000) \end{pmatrix}$$

Note that $\left[\boldsymbol{\Phi}_z^{\mathrm{MC}}\right]_{ij}$ (and $\left[\boldsymbol{\Phi}_z^{\mathrm{MC}}\right]_{ij}$) components are computed using (22)–(22) with $n = 10^7$ and $\rho = 0$. Note also that all these three matrices are symmetric with unitary diagonal terms.

C. Point-Estimate Results

The point-estimate (PE) algorithm, described in Section III-C, is used to determine the processed measurement variance matrix $\boldsymbol{C}_z^{\mathrm{PE}}$ at bus 1. Using (7), correlation coefficient matrix $\boldsymbol{\Phi}_z^{\mathrm{PE}}$ can be easily computed from $\boldsymbol{C}_z^{\mathrm{PE}}$, yielding:

$$\boldsymbol{\Phi}_z^{\mathrm{PE}} = \begin{array}{c} \\ V \\ P \\ P_{1,2} \\ P_{1,3} \end{array} \begin{array}{c} \begin{array}{cccc} V & P & P_{1,2} & P_{1,3} \end{array} \\ \begin{pmatrix} 1.0000 & 0.6126 & 0.4591 & 0.2525 \\ 0.6126 & 1.0000 & 0.2812 & 0.1547 \\ 0.4591 & 0.2812 & 1.0000 & 0.1159 \\ 0.2525 & 0.1547 & 0.1159 & 1.0000 \end{pmatrix} \end{array}$$

Comparing $\boldsymbol{\Phi}_z^{\mathrm{PE}}$ and $\boldsymbol{\Phi}_z^{\mathrm{MC}}$, it is observed that both matrices are remarkably similar. Since $\boldsymbol{\Phi}_z^{\mathrm{PE}}$ and $\boldsymbol{\Phi}_z^{\mathrm{MC}}$ values diverge at fourth decimals, it is proved that point-estimate technique provides precise results, according to the selected accuracy level. Note also that every $\left[\boldsymbol{\Phi}_z^{\mathrm{PE}}\right]_{ij}$ element is comprised within the range defined by $\left[\underline{\boldsymbol{\Phi}_z^{\mathrm{MC}}}\right]_{ij}$ and $\left[\overline{\boldsymbol{\Phi}_z^{\mathrm{MC}}}\right]_{ij}$.

D. Computational Comparison

In this section, Monte Carlo and point-estimate methods are compared from a computational point of view. Table II provides the computational characterization for both techniques. For these simulations, a Linux-based server with four processors clocking at 2.6 GHz and 32 GB of RAM is used.

TABLE II
COMPUTATIONAL COMPARISON BETWEEN MC AND PE METHODS.

Parameters	Monte Carlo				Point Estimate
Sample size	10^4	10^5	10^6	10^7	–
CIW ($\times 10^{-3}$)	39	12	3.9	1.1	–
Time (s)	0.075	0.55	3.95	44.14	0.004
Memory (Mb)	3.618	35.89	358.6	3585	0.02244

Table II shows that point-estimate method clearly outperforms computationally the Monte Carlo technique for every accuracy level.

E. Correlation Study

In this section, the correlation matrices of several buses are compared to illustrate (i) that $\boldsymbol{\Phi}_z$ values are notably dissimilar from one bus to other, and (ii) that these values can be estimated approximately using Fig. 3.

Three buses are considered to highlight several trends. For the purpose of conciseness, we only provide results for one line at each bus. Considered buses are 1, 7, 23, and the lines considered are 1-2, 7-5, 23-24, respectively. Table III provides the voltage, current and phase angle actual values for each line. The last three columns of this table provide the correlation coefficient values computed using the point-estimate technique.

TABLE III
VOLTAGES (P.U.), CURRENTS (P.U.), PHASE ANGLES (RAD), AND CORRELATION COEFFICIENTS.

Bus	Line	V_i	I_{ij}	ψ_{ij}	ρ_{VP}	ρ_{VQ}	ρ_{PQ}
1	1–2	1.0600	0.55	-0.14	0.459	-0.129	-0.213
7	7–5	1.0047	0.06	-0.65	0.062	-0.062	-0.992
23	23–24	1.0045	0.01	0.71	0.007	0.007	1.000

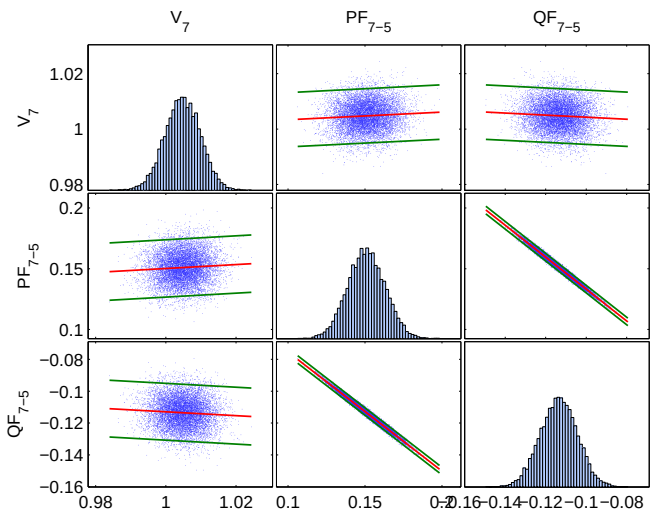

Fig. 6. Graphical study of correlations for line 7-5 at bus 7.

Results from simulating ten thousand measurement scenarios are summarized in Fig. 6. This figure is composed of nine graphics: the diagonal graphics depict each output measurement histogram ($\{V_i, P_{ij}, Q_{ij}\}$); and the non-diagonal graphics are paired, and depict the plot of confronted sample measurement vectors ($\{V_i - P_{ij}, V_i - Q_{ij}, P_{ij} - Q_{ij}\}$). For the non-diagonal graphics the regression line and 95% confidence interval bounds are also plotted.

The following observations are in order:

1) From Fig. 6, it is observed that the correlation between measurements $P_{7,5}$ and $Q_{7,5}$ is high, and can be detected visually. It can be concluded that disregarding the dependency between some measurement pairs is unrealistic.
2) From histograms of Fig. 6, note that the distribution of processed measurements can be considered normal, supporting the traditional assumption about Gaussian-distributed measurement errors.
3) Fig. 3 allow us to estimate the correlation coefficient absolute value in an approximate way, once we know the $\{V_i^f, I_{ij}^f, \psi_{ij}^f\}$ actual values. The accuracy of this procedure is reasonably high. Note that disregarding the voltage value makes no any significant difference.
4) As shown in Table III, if the largest absolute correlation value is low, the rest of the correlation values are significant (as it occurs with line 1–2). This trend can be derived from Fig. 3. On the other hand, if the largest absolute correlation value is high, the rest of the correlation coefficient values are almost insignificant, as shown in Fig. 6 and Table III.
5) From Table III, note that the correlation coefficient value

can be very high and close to one. In this case, the values of other correlation coefficients are approximately zero. Note also that a correlation coefficient absolute value of 1.000 is possible under normal operating conditions in a electric energy system.

VII. Conclusions

Processing current, voltage and power measurements within a substation clearly requires taking into account their statistical dependency. This is particularly relevant to achieve an accurate estimation of the state of an electric energy system through state-estimation algorithms.

The technique provided in this paper allows estimating the correlation matrix of the set of measurements pertaining to a substation. This estimation is carried out using a simple mathematical algorithm - point estimate - that involving low computational burden achieves high accuracy.

The systematic comparison through different case studies of the proposed technique with a cumbersome Monte Carlo algorithm shows the good performance of the technique proposed. Likewise, numerical simulations carried out corroborates the traditional normality assumption whereby measurement errors are considered normal distributed.

Appendix

For the sake of simplicity and without loss of generality, let us consider a vectorial function $\boldsymbol{z} = \boldsymbol{F}(\boldsymbol{p})$ in which both output and input variable vectors $\boldsymbol{z}$ and $\boldsymbol{p}$, respectively, are composed of two components, that is:

$$\boldsymbol{z} = \begin{pmatrix} z_1 \\ z_2 \end{pmatrix}, \quad \boldsymbol{p} = \begin{pmatrix} p_1 \\ p_2 \end{pmatrix}, \quad \begin{pmatrix} z_1 \\ z_2 \end{pmatrix} = \begin{pmatrix} F_1(p_1, p_2) \\ F_2(p_1, p_2) \end{pmatrix}.$$

Likewise, let us assume that input random variables p_1 and p_2 are independent, which can be statistically stated as $E[(p_1 - \mu_{p_1})^i (p_2 - \mu_{p_2})^j] = 0, \forall (i,j) | i \neq j$.

Function $\boldsymbol{F}(\cdot)$ can be expanded in bivariate Taylor series around the mean vector $\boldsymbol{\mu} = (\mu_{p_1}, \mu_{p_2}) = (E[p_1], E[p_2])$. Then, by making use of this series expansion and applying definitions (11) and (12), expectation over the product of variables z_1 and z_2, i.e., $E[z_1 z_2]$, can be expressed as:

$$\begin{aligned} E[z_1 z_2] &= F_1(\boldsymbol{\mu}) F_2(\boldsymbol{\mu}) + F_1(\boldsymbol{\mu}) \sum_{i=1}^{\infty} \frac{1}{i!} \left. \frac{\partial^i F_2}{\partial p_1^i} \right|_{\boldsymbol{\mu}} \lambda_{1,i} \, (\sigma_1)^i \\ &+ F_1(\boldsymbol{\mu}) \sum_{j=1}^{\infty} \frac{1}{j!} \left. \frac{\partial^j F_2}{\partial p_2^j} \right|_{\boldsymbol{\mu}} \lambda_{2,j} \, (\sigma_2)^j \\ &+ F_2(\boldsymbol{\mu}) \sum_{i=1}^{\infty} \frac{1}{i!} \left. \frac{\partial^i F_1}{\partial p_1^i} \right|_{\boldsymbol{\mu}} \lambda_{1,i} \, (\sigma_1)^i \\ &+ F_2(\boldsymbol{\mu}) \sum_{j=1}^{\infty} \frac{1}{j!} \left. \frac{\partial^j F_1}{\partial p_2^j} \right|_{\boldsymbol{\mu}} \lambda_{2,j} \, (\sigma_2)^j \\ &+ \sum_{i=1}^{\infty} \sum_{j=1}^{\infty} \frac{1}{i!j!} \left. \frac{\partial^i F_1}{\partial p_1^i} \right|_{\boldsymbol{\mu}} \left. \frac{\partial^j F_2}{\partial p_1^j} \right|_{\boldsymbol{\mu}} \lambda_{1,i+j} \, (\sigma_1)^{i+j} \\ &+ \sum_{i=1}^{\infty} \sum_{j=1}^{\infty} \frac{1}{i!j!} \left. \frac{\partial^i F_1}{\partial p_2^i} \right|_{\boldsymbol{\mu}} \left. \frac{\partial^j F_2}{\partial p_2^j} \right|_{\boldsymbol{\mu}} \lambda_{2,i+j} \, (\sigma_2)^{i+j}, \end{aligned} \tag{25}$$

where all the terms containing crossed moments of input variables have been eliminated from (25) under the assumption of independency.

On the other hand, the estimate of expectation $E[z_1 z_2]$ given by the two-point estimate method is the one shown in equation (19). This estimate can be also expanded by using univariate Taylor series around the mean vector $\boldsymbol{\mu} = (\mu_{p_1}, \mu_{p_2})$. If the location definition (9) is introduced into this series, the estimate of $E[z_1 z_2]$ can be expressed as:

$$\begin{aligned} E[z_1 z_2] &\cong [w_{11} + w_{12} + w_{21} + w_{22}] F_1(\boldsymbol{\mu}) F_2(\boldsymbol{\mu}) \\ &+ F_1(\boldsymbol{\mu}) \sum_{i=1}^{\infty} \frac{1}{i!} \left. \frac{\partial^i F_2}{\partial p_1^i} \right|_{\boldsymbol{\mu}} [w_{11} \, \xi_{11}^i + w_{12} \, \xi_{12}^i] \, \sigma_1^i \\ &+ F_2(\boldsymbol{\mu}) \sum_{i=1}^{\infty} \frac{1}{i!} \left. \frac{\partial^i F_1}{\partial p_1^i} \right|_{\boldsymbol{\mu}} [w_{11} \, \xi_{11}^i + w_{12} \, \xi_{12}^i] \, \sigma_1^i \\ &+ \sum_{i=1}^{\infty} \sum_{j=1}^{\infty} \frac{1}{i!j!} \left. \frac{\partial^i F_1}{\partial p_1^i} \right|_{\boldsymbol{\mu}} \left. \frac{\partial^j F_2}{\partial p_1^j} \right|_{\boldsymbol{\mu}} [w_{11} \, \xi_{11}^{i+j} + \, w_{12} \, \xi_{12}^{i+j}] \, \sigma_1^{i+j} \end{aligned} \tag{26}$$

And subtracting the above estimate from (25), the estimation error can be cast as follows:

$$\begin{aligned} error &= F_1(\boldsymbol{\mu}) \sum_{i=4}^{\infty} \frac{1}{i!} \left. \frac{\partial^i F_2}{\partial p_1^i} \right|_{\boldsymbol{\mu}} [\lambda_{1,i} - (w_{11} \, \xi_{11}^i + w_{12} \, \xi_{12}^i)] \, \sigma_1^i \\ &+ F_1(\boldsymbol{\mu}) \sum_{i=4}^{\infty} \frac{1}{i!} \left. \frac{\partial^i F_2}{\partial p_2^i} \right|_{\boldsymbol{\mu}} [\lambda_{2,i} - (w_{21} \, \xi_{21}^i + w_{22} \, \xi_{22}^i)] \, \sigma_2^i \\ &+ F_2(\boldsymbol{\mu}) \sum_{i=4}^{\infty} \frac{1}{i!} \left. \frac{\partial^i F_1}{\partial p_1^i} \right|_{\boldsymbol{\mu}} [\lambda_{1,i} - (w_{11} \, \xi_{11}^i + w_{12} \, \xi_{12}^i)] \, \sigma_1^i \\ &+ F_2(\boldsymbol{\mu}) \sum_{i=4}^{\infty} \frac{1}{i!} \left. \frac{\partial^i F_1}{\partial p_2^i} \right|_{\boldsymbol{\mu}} [\lambda_{2,i} - (w_{21} \, \xi_{21}^i + w_{22} \, \xi_{22}^i)] \, \sigma_2^i \\ &+ \sum_{i=1}^{\infty} \sum_{\substack{j=1 \\ i+j>3}}^{\infty} \frac{1}{i!j!} \left. \frac{\partial^i F_1}{\partial p_1^i} \right|_{\boldsymbol{\mu}} \left. \frac{\partial^j F_2}{\partial p_1^j} \right|_{\boldsymbol{\mu}} [\lambda_{1,i+j} - (w_{11} \, \xi_{11}^{i+j} + \, w_{12} \, \xi_{12}^{i+j})] \, \sigma_1^{i+j} \\ &+ \sum_{i=1}^{\infty} \sum_{\substack{j=1 \\ i+j>3}}^{\infty} \frac{1}{i!j!} \left. \frac{\partial^i F_1}{\partial p_2^i} \right|_{\boldsymbol{\mu}} \left. \frac{\partial^j F_2}{\partial p_2^j} \right|_{\boldsymbol{\mu}} [\lambda_{2,i+j} - (w_{21} \, \xi_{21}^{i+j} + w_{22} \, \xi_{22}^{i+j})] \, \sigma_2^{i+j} \end{aligned} \tag{27}$$

Note that, in order to derive (27), the system of equations (10) has been used. Finally, it should be also noted that, for estimation error to be zero, F_1 and F_2 are required to be linear functions. Therefore, it can be concluded that Hong's two-point estimate method provides a linear approximation of the covariance matrix.

References

[1] S. Svensson, "Power measurement techniques for non-sinusoidal conditions," Ph.D. dissertation, Chalmers University of Technology, 1999.

[2] *Multifunction Meter DM9200*, Td ed., Arteche, July 2005. Available on: *http://www.arteche.com/.*

[3] APEC/APLMF Legal Metrology, *Handbook on Electricity Meters*, Tokio, 2006. Available on: *http://www.apec.org/*

[4] International Organization of Legal Metrology, "Electricity Meters", Germany, 2007. *http://www.oiml.org/*

[5] F. C. Schweppe and J. Wildes, "Power system static state estimation. Part I: Exact model," *IEEE Trans. Power App. Syst.*, vol. 89, no. 1, pp. 120–125, Jan. 1970.

[6] F. C. Schweppe and D. Rom, "Power system static state estimation. Part II: Approximate model," *IEEE Trans. Power App. Syst.*, vol. 89, no. 1, pp. 125–130, Jan. 1970.

[7] F. C. Schweppe, "Power system static state estimation. Part III: Implementation," *IEEE Trans. Power App. Syst.*, vol. 89, no. 1, pp. 130–135, Jan. 1970.
[8] R. Larson, W. Tinney, L. Hadju, and D. Piercy, "State estimation in power systems. part ii: Implementations and applications," *IEEE Trans. Power App. Syst.*, vol. 89, no. 3, pp. 353–362, Mar. 1970.
[9] A. Monticelli and A. García, "Fast decoupled state estimators," *IEEE Transa. Power Syst.*, vol. 5, no. 2, pp. 556–564, May 1990.
[10] L. Holten, A. Gjelsvik, S. Aam, F. Wu, and W. H. E. Liu, "Comparison of different methods for state estimation," *IEEE Trans. Power Syst.*, vol. 3, no. 4, pp. 1798–1806, Nov. 1988.
[11] A. Monticelli, "Electric power system state estimation," *Proceedings of the IEEE*, vol. 88, no. 2, pp. 262–282, 2000.
[12] A. Abur and A. G. Expósito, *Electric Power System State Estimation. Theory and Implementations*. New York: Marcel Dekker, 2004.
[13] E. Caro, A. J. Conejo, and R. Mínguez, "A mathematical programming approach to state estimation," in *Optimization Advances in Electric Power Systems*, E. D. Castronuovo, Ed., Nova Science Publishers, Inc., 2008.
[14] E. Rosenblueth, "Point estimates for probability moments," *Proc. Nat. Acad. Sci.*, vol. 72, pp. 3812–3814, Oct. 1975.
[15] ——, "Two-point estimates in probability," *Appl. Math. Model.*, vol. 5, pp. 329–335, Oct. 1981.
[16] S. S. Hyun and M. K. Byung, "Efficient statistical tolerance analysis for general distributions using three-point information," *Int. J. Prod. Res.*, vol. 40, no. 4, pp. 931–944, 2002.
[17] K. S. Li, "Point-estimate method for calculating statistical moments," *J. Eng. Mech.-ASCE* , vol. 118, no. 7, pp. 1506–1511, 1992.
[18] C. W. Tsai and S. Franceschini, "Evaluation of probabilistic point estimate methods in uncertainty analysis for environmental engineering applications," *J. Environ. Eng.-ASCE* , vol. 131, no. 3, pp. 387–395, 2005.
[19] W. Liping, D. Beeson, and G. Wiggs, "Efficient and accurate point estimate method for moments and probability distribution estimation," in *10th AIAA/ISSMO Multidisciplinary Analysis and Optimization Conference*, Albany, New York, 30 August-1 September 2004.
[20] M. E. Harr, "Probabilistic estimates for multivariate analysis," *Appl. Math. Model.*, vol. 13, no. 5, pp. 313–318, 1989.
[21] H. P. Hong, "An efficient point estimate method for probabilistic analysis," *Reliab. Eng. Syst. Saf.*, vol. 59, pp. 261–267, 1998.
[22] C.-L. Su, "Probabilistic load-flow computation using point estimate method," *IEEE Trans. Power Syst.*, vol. 20, no. 4, pp. 1843–1851, Nov. 2005.
[23] C.-L. Su and C.-N. Lu, "Two-point estimate method for quantifying transfer capability uncertainty," *IEEE Trans. Power Syst.*, vol. 20, no. 4, pp. 1843–1851, Nov. 2005.
[24] J. M. Morales and J. Pérez-Ruiz, "Point estimate schemes to solve the probabilistic power flow," *IEEE Trans. Power Syst.*, vol. 22, no. 4, pp. 1594–1601, Nov. 2007.
[25] G. Verbič and C. A. Cañizares, "Probabilistic optimal power flow in electricity markets based on a two-point estimate method," *IEEE Trans. Power Syst.*, vol. 21, no. 4, pp. 1883 – 1893, Nov. 2006.
[26] R. Y. Rubinstein, *Simulation and the Monte Carlo Method*. New York: Wiley, 1981.
[27] H. Hotelling, *New light on the correlation coefficient and its transforms*. Journal of the Royal Statistical Society B, 1953, vol. 15.
[28] Power Systems Test Case Archive. Available on: *http://www.ee.washington.edu/research/pstca/*

Eduardo Caro received from the Polytechnical University of Cataluña, Barcelona, Spain, the Electrical Engineering degree in June 2007. He is currently a Ph.D. student at the University of Castilla-La Mancha, Ciudad Real, Spain.

His research interests include power system state estimation, optimization, sensitivity analysis, and power system quality.

Juan M. Morales (S'07) received the Ingeniero Industrial degree from the Universidad de Málaga, Spain, in 2006. He is currently working toward the Ph.D. degree at the Universidad de Castilla-La Mancha.

His research interests are in the fields of power systems economics, reliability, stochastic programming and electricity markets.

Antonio J. Conejo (F'04) received the M.S. degree from MIT, Cambridge, MA, in 1987, and a Ph.D. degree from the Royal Institute of Technology, Stockholm, Sweden in 1990. He is currently a full Professor at the Universidad de Castilla-La Mancha, Ciudad Real, Spain.

His research interests include control, operations, planning and economics of electric energy systems, as well as statistics and optimization theory and its applications.

Roberto Mínguez received from the University of Cantabria, Santander, Spain, the Civil Engineering degree, and the Ph.D. degree in Applied Mathematics and Computer Science in September 2000 and June 2003, respectively. During 2004 he worked as Visiting Scholar at Cornell University, New York, under the Fulbright program. He is currently an Assistant Professor of Environmental Hydraulics Institute IH, Universidad de Cantabria, Cantabria.

His research interests are reliability engineering, sensitivity analysis, numerical methods, and optimization.